DOI: 10.1002/ejic.200500939

Synthesis, Crystal Structures, and Photophysical Properties of Two Novel Lead(II)–SIP Coordination Polymers (NaH_2SIP = 5-Sulfoisophthalic Acid Monosodium Salt) Containing Tetranuclear Lead(II) Units

Qing-Yan Liu[a,b] and Li Xu*[a]

Keywords: Tetranuclear lead / Hydrothermal synthesis / Crystal structures / Photophysical properties

Two new Pb^{II}–SIP coordination polymers, $\{[Pb_4(OH)_2(SIP)_2(H_2O)](H_2O)_5\}_n$ (**1**) and $[Pb_3(SIP)_2(H_2O)_5]_n$ (**2**), have been synthesized by hydrothermal reactions of $Pb(OH)_2$ or $Pb(NO_3)_2$ and 5-sulfoisophthalic acid monosodium salt (NaH_2SIP) at 160 °C, respectively. Single-crystal X-ray diffraction reveals that compound **1** has a 2D brick-wall-like architecture constructed from 1D tapes containing the basketlike tetranuclear $[Pb_4(\mu_3\text{-}OH)_2(COO)_2]$. Compound **2** has a 2D-layered structure, which is constructed from a 1D-ladder structure composed of the cyclic $[Pb_4(SIP)_2(COO)_2]$ grid with the four Pb atoms nearly coplanar. In the solid state, compound **1** exhibits blue photoluminescence with the maximum emission intensity at 436 nm upon excitation at 335 nm. Compound **2** shows phosphorescence with the maximum emission intensity at 603 nm upon excitation at 426 nm. Both compounds have also been characterized by elemental analysis, IR spectra, TG analysis, and powder X-ray diffraction.

Introduction

The design and construction of coordination polymers is one of the most active areas of materials research. The intense interest in these materials is driven by both their interesting network topologies and potential applications such as catalysis, molecular magnets, sensors, ion exchange, adsorption, and phase separation.[1–4] Many of the efforts have so far been devoted to the study of transition-metal-based coordination polymers.[5–7] However, relatively little attention has been paid to the coordination polymers of main group metal ions despite their important applications in electroluminescent devices or organic light-emitting diode (OLED) technology.[8–11] Pb^{2+} is employed in the present work for several reasons: (1) it has a $6s^2$ outer electron configuration and large radius, which can lead to interesting topological arrangements;[12–14] (2) the absence of crystal field stabilization energy effects allows the Pb^{2+} ion to adopt varied coordination geometries including octahedra, tetrahedra, or square planes amongst others, which give rise to novel coordination networks;[15–17] and (3) it has interesting photochemical and photophysical properties.[18–21] On the other hand, the SIP ligand, with three functional groups, exhibits multiple coordinating modes facilitating the formation of multi-dimensional structures and diversified topologies.[22–24] Recently, we have reported a series of lanthanide–SIP coordination polymers wherein SIP proves to be a sensitive probe in examining the role of the lanthanide contraction effect in crystal structure formation.[25] In this contribution, SIP will serve as a probe to examine the coordination polymer chemistry of Pb^{2+}, and the two novel polymeric materials with Pb_4 secondary building blocks, $\{[Pb_4(OH)_2(SIP)_2(H_2O)](H_2O)_5\}_n$ (**1**) and $[Pb_3(SIP)_2(H_2O)_5]_n$ (**2**), will be described with regard to syntheses, crystal structures, TG analysis, powder X-ray diffraction, IR spectra, and photoluminescent properties. An unprecedented coordinating mode of SIP (Scheme 1, b) is observed in polymer **1**.

Results and Discussion

Preparation of the Complexes

Hydrothermal synthesis is widely employed to produce new structures, but is still a kind of "black box". This method can minimize the problems associated with ligand solubility and enhance the reactivity of reactants in favor of efficient molecular building during the crystallization process. The two Pb^{II}–SIP polymers, $\{[Pb_4(OH)_2(SIP)_2(H_2O)](H_2O)_5\}_n$ (**1**) and $[Pb_3(SIP)_2(H_2O)_5]_n$ (**2**), are obtained from hydrothermal reactions of the lead(II) salts and NaH_2SIP in aqueous solution. The preparative reactions

[a] State Key Laboratory of Structural Chemistry, Fujian Institute of Research on the Structure of Matter, Chinese Academy of Sciences,
Fuzhou, Fujian, 350002, P. R. China
Fax: +86-591-83705045
E-mail: xli@fjirsm.ac.cn
[b] Graduate School of the Chinese Academy of Sciences,
Beijing 100039, P. R. China
Fax: +86-591-83705045
E-mail: qyliu@fjirsm.ac.cn

Supporting information for this article is available on the WWW under http://www.eurjic.org or from the author.

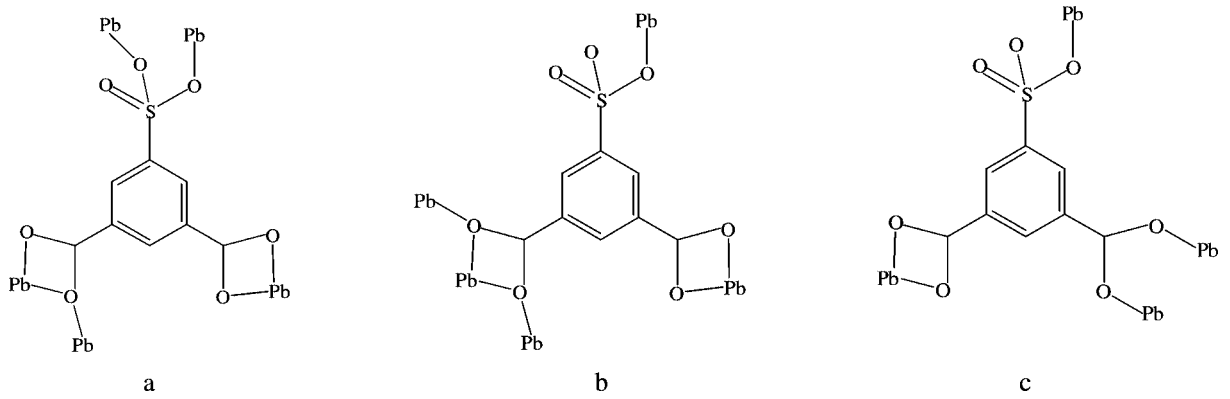

Scheme 1. Coordination modes of SIP observed in compound **1** and **2**.

were carried out under different temperatures (140, 160, and 180 °C) to examine the temperature-dependence of their solid structures. X-ray diffraction analyses of the reaction products indicate that the same results were obtained under these reaction temperatures although the purity and yields are slightly different, indicative of the thermodynamic nature of the hydrothermal reactions. Compounds **1** and **2** cannot be obtained from the reaction of the corresponding lead(II) salts and NaH_2SIP in aqueous solution at room temperature (in contrast to hydrothermal conditions), indicating the kinetic nature of this conventional method. The dramatic difference in reaction products between conventional and hydrothermal reactions is attributable to their different reaction mechanisms that are shifted from a kinetic domain for conventional solution reactions to a thermodynamic domain for hydrothermal reactions.[26–28]

Crystal Structure of $\{[Pb_4(OH)_2(SIP)_2(H_2O)](H_2O)_5\}_n$ (1)

Compound **1** features a two-dimensional brick-wall-like architecture constructed from unusual tetranuclear lead(II) motifs as a secondary building block. As depicted in Figure 1 (a), the asymmetric unit of **1** contains four crystallographically independent lead(II) ions. Pb(1) is surrounded by six oxygen atoms, of which four are from three surrounding SIP ligands, one is from a water molecule, and one is from a μ_3-hydroxy group. The coordination geometry of Pb(1) can be described as a distorted pentagonal bipyramid with the seventh coordination site occupied by its lone pair of electrons. The atoms O(17) and O(6B) (B: $-x + 1$, $y + 1/2$, $-z + 2/3$) occupy the axial positions (Figure 1, a). The Pb(1)–O distances range from 2.469(8) to 2.714(8) Å, comparable to those observed in the related lead(II) compounds.[7–9] The Pb(3) atom has a similar coordination geometry to that of Pb(1) with the two apical positions occupied by the carboxylate and hydroxy oxygen atoms [O(2E) (E: $-x + 1$, $y - 1/2$, $-z + 3/2$) and O(16)], and they both have similar Pb–O distances [Pb–O = 2.425(8)–2.752(8) Å]. Pb(2) has a distorted [:PbO4] tetragonal-pyramid geometry with the four basal positions occupied by a chelating carboxylate group and two μ_3-hydroxy groups and the apical position occupied by the lone pair of electrons. The Pb(2)–O distances [2.328(8)–2.612(9) Å] are slightly shorter than those around the six-coordinate Pb(1) center. The Pb(4) atom has a similar coordination geometry to that of Pb(2) as illustrated in Figure 1 (a). As shown in Figure 1 (b), the four Pb^{2+} ions are capped by two μ_3-hydroxy groups generating a butterfly $[Pb_4(\mu_3\text{-}OH)_2]$ cluster. The Pb(1)Pb(2) Pb(3) and Pb(1)Pb(4)Pb(3) triangles are each capped by an additional carboxylate group to form a basketlike structure with a weak Pb(1)–O(4) (3.18 Å) interaction. The basal plane [Pb(2), Pb(4), O(15), and O(16)] of the basket is almost planar with the Pb(4)–O(15)–Pb(2) and Pb(4)–O(16)–Pb(2) angles of 104.6(3) and 103.1(3)°, respectively (Table 1). The Pb(2)···Pb(4) separation of about 3.8 Å is longer than the sum of the van der Waals radii (3.20 Å).[29] The dihedral angles between the side faces and the basal plane are 67.8(2), 97.2(1), 112.8(2), 106.1(1), 88.2(1), and 64.8(3)°, respectively. Interestingly, the basketlike structure of the tetranuclear cluster $[Pb_4(\mu_3\text{-}OH)_2(COO)_2]$ core resembles many cubanelike structures that are commonly found in many other compounds. However, in the current compound the carboxylate groups make the cluster more open instead of the bridging oxygen atoms.[30–31] Several complexes containing $[Pb_4(\mu_3\text{-}OH)_2]$ have been documented, but the $[Pb_4(\mu_3\text{-}OH)_2]$ cluster has a chair structure with the two Pb atoms above and below the $[Pb_2(\mu_3\text{-}OH)_2]$ plane.[32–34] Therefore, this is a rare example concerning lead(II) complexes.

As shown in Figure 1 (a), the two independent SIP ligands exhibit different coordinating modes. SIP(a) acts as a pentadentate ligand (Scheme 1, a) with the bidentate sulfonate group, one chelating carboxylate group, and one μ_2-η^2:η^1 carboxylate group (one oxygen atom bridges two metal atoms, the other connects one metal atom, and the carboxylate group coordinates to two metal atoms). The unprecedented coordinating mode of SIP(b) is depicted in Scheme 1 (b) wherein one carboxylate group chelates to one Pb^{2+} ion and the other displays an unusual μ_3-η^2:η^2 coordinating mode (each oxygen atom coordinates to two metal atoms and the carboxylate group coordinates to three metal atoms). To the best of our knowledge, this type of coordinating mode of the SIP ligand is not observed in the previously reported SIP complexes. Unlike that of SIP(a), the sulfonate group of the SIP(b) ligand is unidentate.

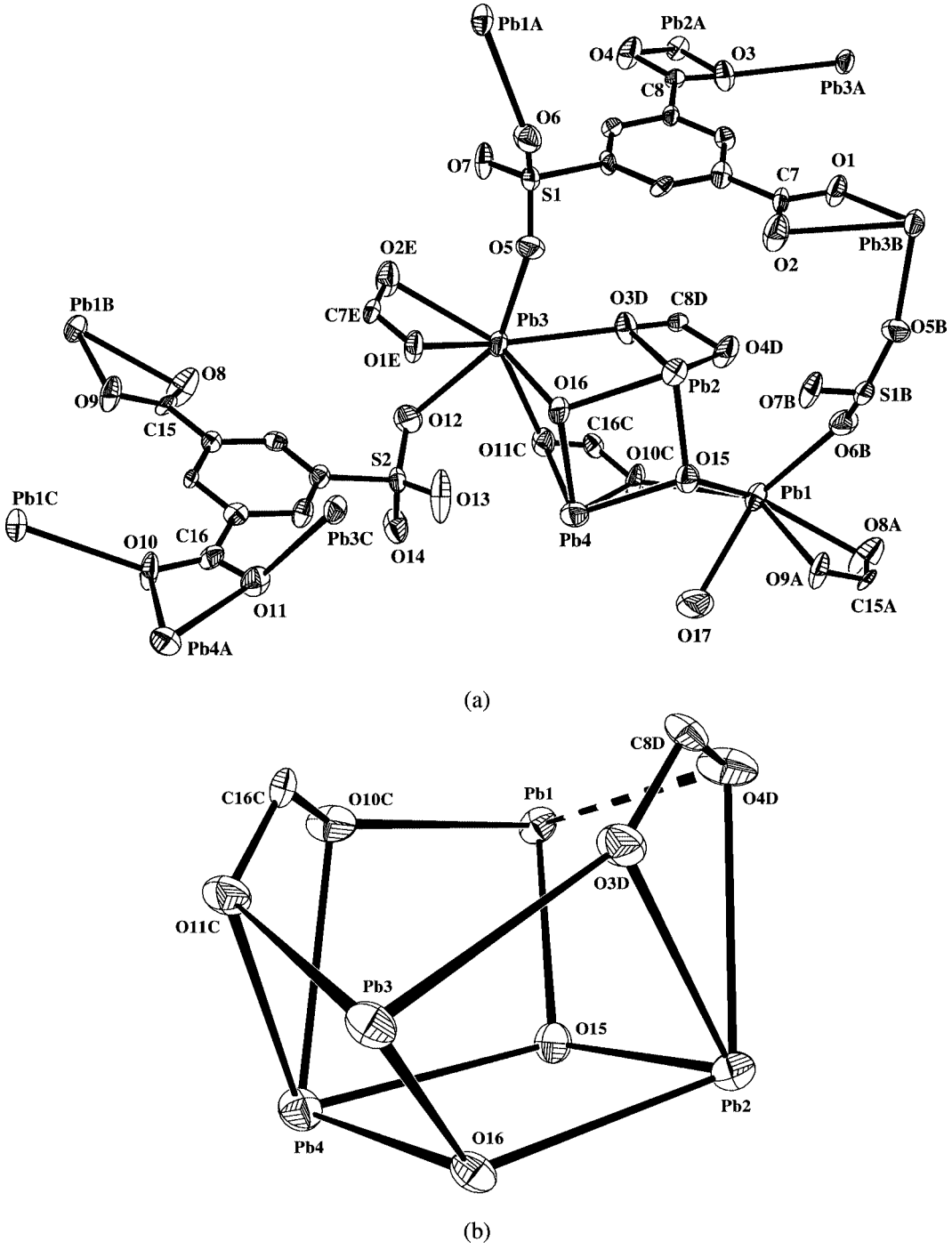

Figure 1. (a) Molecular structure of compound **1**. (b) The basketlike tetranuclear $[Pb_4(\mu_3\text{-}OH)_2(COO)_2]$ cluster as a secondary building block.

The $[Pb_4(\mu_3\text{-}OH)_2(COO)_2]$ secondary building blocks are interconnected into a one-dimensional tape structure propagating along the crystallographic *b* axis (Figure 2) by the SIP ligand through the chelating carboxylate and sulfonate groups. Two types of 16-membered rings are observed in the 1D tape; ring A is composed of two SIP ligands and two Pb atoms and ring B consists of one $[Pb_4(\mu_3\text{-}OH)_2(COO)_2]$, one Pb atom, one SIP ligand, and one sulfonate group. Such cyclic structures are characteristic of the SIP coordination polymers.[25] The separation between the two neighboring Pb_4 units, linked by ring A, is 15.3 Å, comparable to the length of the *b* axis. As described above, the two independent SIP ligands use four of their six functional groups to form a 1D tape. The remaining two carboxylate groups link the 1D tapes along the *c* axis into a 2D brick-wall-like layered structure where the cavities have an approximate dimension of 12.8×6.5 Å, as depicted in Figure 3. The layers are parallel and do not slip in the crystal

Table 1. Selected bond lengths [Å] and bond angles [°] of **1**.

Pb(1)–O(8A)	2.676(9)	Pb(1)–O(9A)	2.482(8)
Pb(1)–O(10C)	2.714(8)	Pb(1)–O(15)	2.469(8)
Pb(1)–O(17)	2.623(11)	Pb(1)–O(6B)	2.574(8)
Pb(2)–O(3D)	2.525(8)	Pb(2)–O(4D)	2.612(9)
Pb(2)–O(15)	2.328(8)	Pb(2)–O(16)	2.500(8)
Pb(3)–O(1E)	2.440(8)	Pb(3)–O(2E)	2.715(9)
Pb(3)–O(3)	2.752(8)	Pb(3)–O(5)	2.579(8)
Pb(3)–O(11C)	2.687(8)	Pb(3)–O(12)	2.730(10)
Pb(3)–O(16)	2.425(8)	Pb(4)–O(10C)	2.567(8)
Pb(4)–O(11C)	2.490(8)	Pb(4)–O(15)	2.513(8)
Pb(4)–O(16)	2.393(8)		
O(15)–Pb(1)–O(9A)	83.5(3)	O(15)–Pb(1)–O(6B)	91.2(3)
O(15)–Pb(1)–O(10C)	67.8(3)	O(15)–Pb(1)–O(17)	81.6(4)
O(8A)–Pb(1)–O(9A)	50.1(3)	O(8A)–Pb(1)–O(10C)	149.2(3)
O(17)–Pb(1)–O(9A)	74.8(4)	O(17)–Pb(1)–O(8A)	90.8(4)
O(17)–Pb(1)–O(10C)	67.9(3)	O(9A)–Pb(1)–O(6B)	77.4(3)
O(8A)–Pb(1)–O(6B)	74.3(3)	O(10C)–Pb(1)–O(6B)	134.0(3)
O(17)–Pb(1)–O(6B)	151.9(4)	O(3D)–Pb(2)–O(4D)	50.1(3)
O(3D)–Pb(2)–O(16)	69.1(3)	O(15)–Pb(2)–O(16)	76.7(3)
O(15)–Pb(2)–O(4D)	80.1(3)	O(4D)–Pb(2)–O(16)	110.1(3)
O(3D)–Pb(2)–O(15)	97.4(3)	O(1E)–Pb(3)–O(2E)	50.1(3)
O(3D)–Pb(3)–O(2E)	142.7(3)	O(1E)–Pb(3)–O(12)	74.8(3)
O(2E)–Pb(3)–O(12)	73.2(3)	O(16)–Pb(3)–O(1E)	84.1(3)
O(11C)–Pb(3)–O(12)	67.1(3)	O(16)–Pb(3)–O(3D)	66.5(2)
O(3D)–Pb(3)–O(11C)	72.6(3)	O(16)–Pb(3)–O(11C)	70.6(3)
O(5)–Pb(3)–O(2E)	78.2(3)	O(5)–Pb(3)–O(1E)	77.5(3)
O(5)–Pb(3)–O(16)	85.7(3)	O(5)–Pb(3)–O(3D)	72.1(3)
O(11C)–Pb(4)–O(16)	74.6(3)	O(15)–Pb(4)–O(16)	75.3(3)
O(11C)–Pb(4)–O(15)	104.5(3)	O(16)–Pb(4)–O(10C)	100.4(3)
O(11C)–Pb(4)–O(10C)	51.0(2)	O(10C)–Pb(4)–O(15)	69.5(3)
Pb(1)–O(15)–Pb(2)	119.5(3)	Pb(4)–O(15)–Pb(2)	104.6(3)
Pb(1)–O(15)–Pb(4)	110.3(3)	Pb(4)–O(16)–Pb(3)	110.6(3)
Pb(4)–O(16)–Pb(2)	103.1(3)	Pb(3)–O(16)–Pb(2)	114.6(3)

Symmetry transformation for equivalent atoms: A: x, $y + 1$, z; B; $-x + 1$, $y + 1/2$, $-z + 3/2$; C: x, $y - 1$, z; D: $-x + 1$, $-y$, $-z + 1$; E: $-x + 1$, $y - 1/2$, $-z + 3/2$

packing. So, the intralayer pores form a channel along the *a* axis. The lattice water molecules occupying the voids of the 2D layered structure serve as receptors or donors of the extensive O–H···O hydrogen bonds with O···O distances of 2.701(1)–3.096(3) Å. The layers are further held together by π-stacking interactions between the parallel neighboring phenyl rings with a face-to-face distance of 3.337(3) Å, and the neighboring phenyl rings have a dihedral angle of 8.2(1)° with a centroid–centroid distance of 3.728(4) Å. Similar π–π stacking interactions have also been reported in a number of cadmium– and copper–SIP complexes.[35,36]

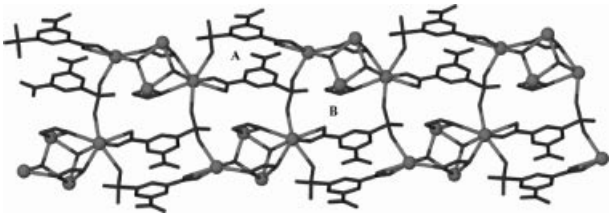

Figure 2. View of the tetranuclear $[Pb_4(\mu_3\text{-}OH)_2(COO)_2]$ bridged by SIP to form a one-dimensional tape structure propagating along the *b* axis (Pb atoms are represented as balls).

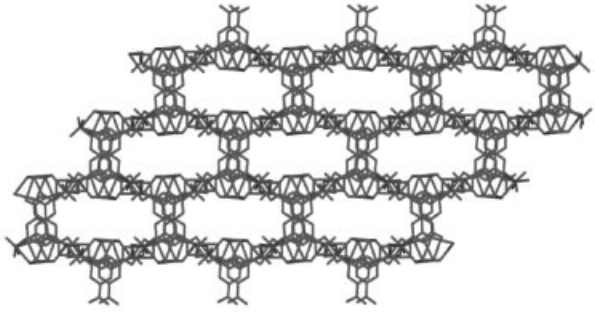

Figure 3. View of the two-dimensional brick-wall-like architecture of **1** along the *bc* plane.

Crystal Structure of $[Pb_3(SIP)_2(H_2O)_5]_n$ (2)

Compound **2** has a 2D-layered structure with the tetranuclear $[Pb_4(SIP)_2(H_2O)_6]$ unit. As shown in Figure 4, the asymmetric unit of **2** consists of three Pb^{2+} ions, two SIP ligands, and five coordinating water molecules. The Pb(1) atom coordinates to three carboxylate oxygen atoms from two SIP ligands and two water molecules, with Pb(1)–O distances of 2.460(15)–2.680(14) Å. The coordination geometry of Pb(1) can be described as a distorted pentagonal

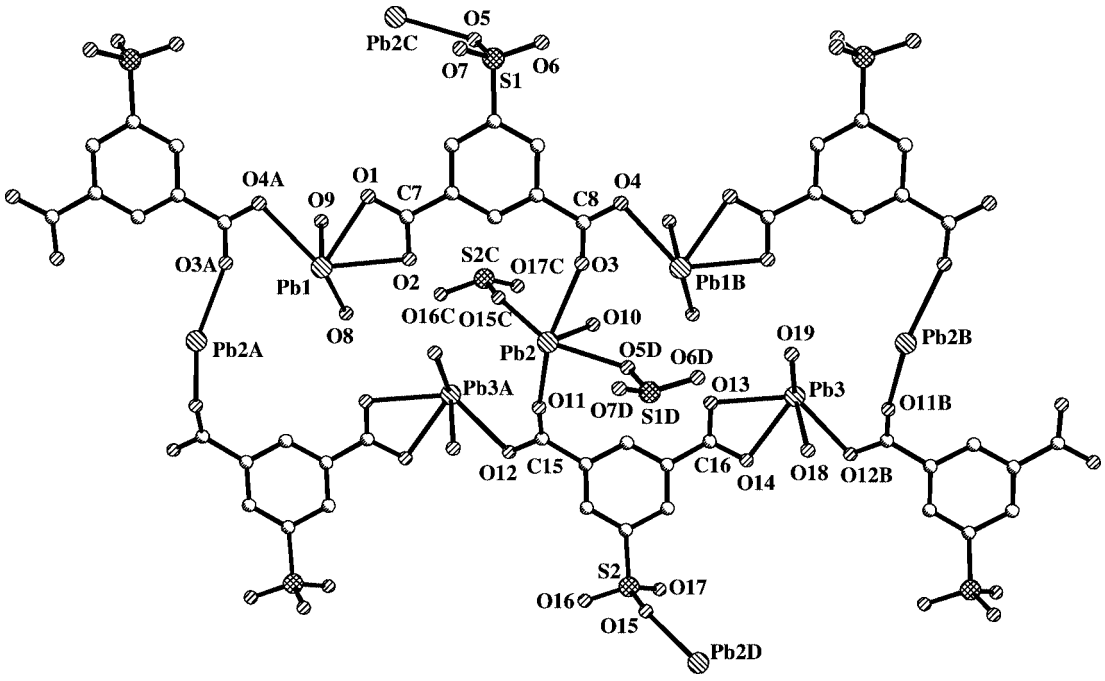

Figure 4. Crystal structure of compound **2**.

pyramid with the lone pair of electrons completing the pentagonal plane and the water molecule [O(9)] lying at the apical position. Pb(3) is crystallographically independent but geometrically similar to Pb(1) with the apical position occupied by the O(18) atom of the water molecule. The Pb(3)–O distances of 2.437(13)–2.715(15) Å are similar to those around Pb(1). Pb(2) has a distorted [:PbO5] octahedral coordination geometry with equatorial positions occupied by two carboxylate and two sulfonate oxygen atoms, and the apical positions taken up by one water molecule and the lone pair of electrons. The Pb(2)–O distances [2.26(2)–2.562(13) Å] are within the normal experimental limitation (Table 3)[12,13] but slightly shorter than those around the seven-coordinate Pb(1) and Pb(3) atoms. The two independent SIP ligands have similar coordinating modes as illustrated in Scheme 1 (c).

As illustrated in Figure 5, the Pb^{2+} ions are interconnected by the SIP ligands into a 1D-ladder structure featuring the cyclic $[Pb_4(SIP)_2(COO)_2]$ with an approximate dimension of 10.2×5.8 Å^2. The four Pb ions [Pb(1), Pb(2), Pb(3A), and Pb(2A), A: x, $y + 1$, z] are nearly coplanar with a maximum deviation of 0.377(1) Å for [Pb(1)] and a mean deviation of 0.344(1) Å. This type of coplanar Pb_4 unit is, to the best our knowledge, uncommon. The 1D ladder can also conveniently be regarded as resulting from two 1D $[Pb(SIP)(H_2O)_2]_n$ single chains bridged by Pb(2) (Figure 5). As mentioned above, the SIP ligands use the carboxylate groups to form the 1D ladder. The remaining sulfonate groups further link the 1D ladders into a 2D layer through Pb(2)–sulfonate bonding [Pb(2)–O(5D), 2.452(15); Pb(2)–O(15C), 2.511(14) Å; C: x, $y - 1$, z, D: x, $y + 1$, z] (see Figure 6). The stacking of the 1D ladders is clearly affected by π interactions between the SIP ligands. The phenyl rings between the ladders are almost parallel and closely stacked [the dihedral angle is 1.5(1)° and the centroid–centroid distance is 3.559(1) Å]. The coordinating water molecules fill the cavities of the neighboring ladders preventing interpenetration.

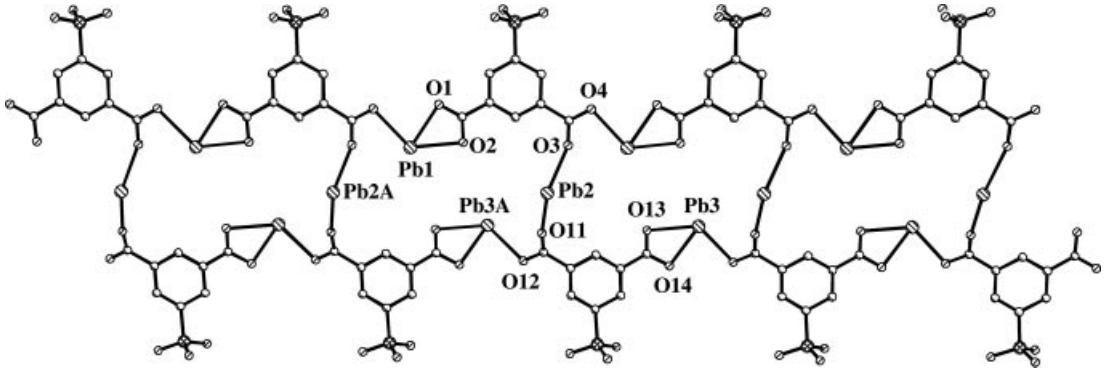

Figure 5. View of the 1D ladder of compound **2** along the *a* axis (water molecules are omitted for clarity).

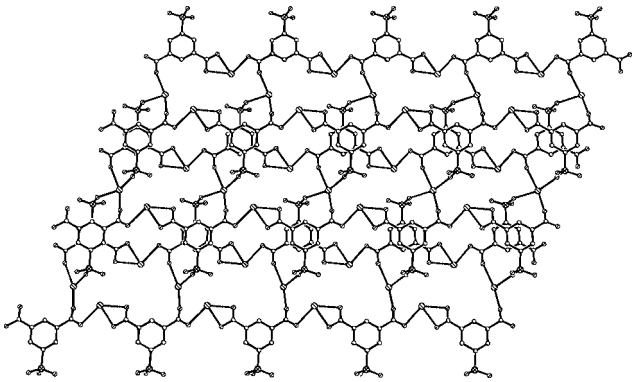

Figure 6. View of the 2D layered structure of **2** in the *ab* plane (water molecules are omitted for clarity).

FT-IR Spectra, Thermogravimetric Analyses, and Powder X-ray Diffraction

The FT-IR spectra of **1** and **2** exhibit broad absorptions centered at 3390 and 3410 cm^{-1} for **1** and **2**, respectively, occurring because of the existence of water molecules in the structures. The IR spectrum of **1** shows the typical asymmetric (1597 cm^{-1}) and symmetric (1542 and 1431 cm^{-1}) stretching bands of carboxylate groups. The respective values of [$\nu_{as}(CO_2) - \nu_s(CO_2)$] clearly indicate the presence of chelating (55 cm^{-1}) and bridging (166 cm^{-1}) coordination modes of the carboxylate groups in **1**.[37] The strong bands at 1598 cm^{-1}, and 1522 and 1434 cm^{-1}, respectively, correspond to the asymmetric and symmetric stretching bands of the carboxylate groups in the IR spectrum of **2**. Similar to those in **1**, the values of [$\nu_{as}(CO_2) - \nu_s(CO_2)$] are 76 cm^{-1} and 164 cm^{-1} in **2**, which supports the presence of chelating and bridging coordination modes of the carboxylate groups. The absorptions in the region 1000–1200 cm^{-1} for the two complexes are typical of the sulfonate group. The strong absorption bands at 621 and 623 cm^{-1} for **1** and **2**, respectively, are because of the ν_{S-O} stretching.

To examine the thermal stability of the two compounds and their structural variation as a function of the temperature, thermogravimetric analyses (TGA) were performed on single-phase polycrystalline samples of these materials (see Figure S1 in the Supporting Information). Results from the TGA measurements of **1** exhibit two distinct weight loss steps. The first weight loss occurs between 60 and 290 °C because of the release of all water molecules (weight loss: measured 7.2%, theoretical 7.4%). The need for such an unusually high temperature for the removal of the water molecules is because of the hydrogen bonding with the carboxylate or sulfonate oxygen atoms. The second weight loss in the temperature range 410–800 °C corresponds to the decomposition of the SIP ligand. The thermogravimetric analysis of **2** shows that the initial weight loss occurs in the temperature range 110–240 °C, attributable to the release of all coordinating water molecules (observed, 7.3%, calculated 7.5%). Increasing the temperature led to the decomposition of the SIP ligand at 420 °C.

The X-ray powder diffraction patterns (XRPD) of both compounds are illustrated in Figure S2 and S3. The different structures of compounds **1** and **2** have also been indicated by their different XRPD patterns. Their XRPD patterns are in good agreement with those simulated from single crystal structural data, thus both compounds **1** and **2** were obtained as a single phase.

Photoluminescent Properties

Photoluminescent properties of s^2-metal complexes are not well studied as compared with those of d^{10}-metal complexes, although there are reports on the photoluminescent properties of lead-containing materials.[38–41] The photoluminescence properties of **1** and **2**, as well as the free ligand, were examined in the solid state at room temperature. The free Na_2HSIP displays photoluminescent emission at 320 nm under 286 nm radiation.[42] Compound **1** exhibits intense photoluminescent emission with a maximum at 436 nm upon excitation at 335 nm (Figure 7). In the case of **2**, photoluminescence with a maximum emission at 603 nm upon excitation at 426 nm is observed. The emission wavelength of **1** (436 nm) is much longer than that of the free SIP ligand (320 nm) and similar to those of the reported s^2-metal cluster complexes.[43–46] Therefore, this emission can be assigned to the lead(II) cluster complex. A remarkable bathochromic shift is also observed in compound **2**. As seen from Figure 7, the emission of **2** occurs at a much lower energy of 603 nm with a large Stokes shift. The low-energy emissions associated with large Stokes shifts have been commonly observed for other s^2-metal complexes, which can be assigned to a metal-centered transition involving the s and p metal orbital as proposed by Vogler.[39,43,47] With these concerns in mind, the emission band at 603 nm of **2** can be assigned to a metal-centered s → p transition. The large Stokes shift is caused by the elimination of the ground-state distortion in the excited state.[39] The further lifetime measurements at room temperature of each emission maximum give the results of 2.43 ns for **1** and 3.47 μs for **2**. The long emission lifetime of **2** can be assigned to phosphorescence, which is consistent with the general idea that the appearance of a room-temperature phosphorescence requires the presence of a heavy metal ion, which re-

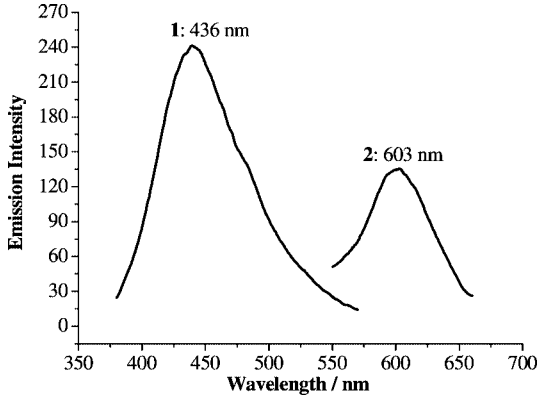

Figure 7. The solid-state emission photoluminescent spectra of **1** (λ_{ex} = 335 nm) and **2** (λ_{ex} = 426 nm) at room temperature.

duces the radiative lifetime of triplets by increased spin-orbit coupling.[21] As described above, we can conclude that the different emission spectra of **1** and **2** can be significantly influenced by their crystal structures.

Conclusion

In conclusion, the self-assembly of the lead(II) ions with SIP affords two novel Pb^{II}–SIP coordination polymers **1** and **2** containing tetranuclear lead(II) motifs. Because of the diversity of the SIP ligand in bridging metal ions, the metal–SIP complexes are expected to show various novel, interesting structures and desired properties. In the present case, compounds **1** and **2**, obtained with the same SIP ligand and under almost the same synthetic procedures, are distinct from each other, with regard to composition, topology, and photoluminescent properties. Compound **1** displays a 2D brick-wall-like structure featuring a unique basketlike tetranuclear $[Pb_4(\mu_3\text{-}OH)_2(COO)_2]$ motif. Compound **2** has a 2D layered structure containing 1D ladders characteristic of the cyclic $[Pb_4(SIP)_2(COO)_2]$ unit. Therefore, the multiple coordinating modes of the SIP ligand, together with the varied coordination geometry of Pb^{2+}, exhibit diverse structural topologies of the Pb^{II}–SIP system. In addition, the lone pair of electrons usually leads to the asymmetric coordination geometry of Pb^{II}, which probably disfavors the formation of high-dimensional structures. So, lead(II) materials usually have low-dimensional structures. Compound **1** displays fluorescent emission and **2** shows phosphorescence emission at room temperature, indicating structure-dependent photoluminescent properties of the Pb–SIP coordination polymers, and revealing potential for application in OLED technology.

Experimental Section

General Remarks: 5-Sulfoisophthalic acid monosodium salt (Alfa) was purchased commercially and used without further purication. Elemental analyses were carried out with an Elementar Vario EL III analyzer and IR spectra (KBr pellets) were recorded with a PerkinElmer Spectrum One. Fluorescent spectra were measured at room temperature with an Edinburgh FL-FS90 TCSPC system. The thermogravimetric measurements were performed with a Netzsch STA449C apparatus under a nitrogen atmosphere with a heating rate of 10 °C/min from 25 to 800 °C. X-ray powder diffraction patterns were performed with a RIGAKU DMAX2500PC diffractometer using Cu-K_α radiation. All complexes were synthesized by the hydrothermal method under autogenous pressure.

Synthsis of $\{[Pb_4(OH)_2(SIP)_2(H_2O)](H_2O)_5\}_n$ (1): A mixture of $Pb(OH)_2$ (0.048 g, 0.2 mmol) and 5-sulfoisophthalic acid monosodium salt (0.027 g, 0.1 mmol) in a 2:1 molar ratio in H_2O (18 mL) was introduced into a Parr Teon-lined stainless steel vessel (30 mL). The vessel was sealed and heated to 160 °C. This temperature was kept for 5 d and then the mixture was cooled at a rate of 5 °C/h to form colorless crystals of **1**. A pale yellow crystalline product was filtered, washed with distilled water, and dried at ambient temperature (yield: 0.47 g, 64% on the basis of Pb). $C_{16}H_{20}O_{22}S_2Pb_4$ (1457.20): calcd. C 13.18, H 1.37; found C 13.11, H 1.33. IR (KBr): $\tilde{\nu}$ = 3390 (s), 1597 (vs), 1542 (vs), 1431(s), 1355 (vs), 1197 (s), 1149 (s), 1107 (s), 1036 (s), 925 (w), 872 (w), 771 (m), 719(s), 677 (w), 621 (s), 447 (m) cm^{-1}.

Synthsis of $[Pb_3(SIP)_2(H_2O)_5]_n$ (2): A mixture of $Pb(NO_3)_2$ (0.033 g, 0.1 mmol), 5-sulfoisophthalic acid monosodium salt (0.041 g, 0.15 mmol), and triethyl amine (0.1 mL) in a 2:3:6 molar ratio in H_2O (18 mL) was introduced into a Parr Teon-lined stainless steel vessel (30 mL). The vessel was sealed and heated to 160 °C. This temperature was kept for 5 d and then the mixture was cooled at a rate of 5 °C/h to form colorless crystals of **1**. A pale yellow crystalline product was filtered, washed with distilled water, and dried at ambient temperature (yield: 0.40 g, 56% on the basis of Pb). $C_{16}H_{16}O_{19}S_2Pb_3$ (1197.98): calcd. C 16.04, H 1.35; found C 16.01, H 1.34. IR (KBr): $\tilde{\nu}$ = 3410 (s), 1598 (vs), 1522 (vs),

Table 2. Selected bond lengths [Å] and bond angles [°] of **2**.

Pb(1)–O(1)	2.468(14)	Pb(1)–O(2)	2.501(14)
Pb(1)–O(8)	2.680(14)	Pb(1)–O(9)	2.460(15)
Pb(1)–O(4A)	2.558(13)	Pb(2)–O(3)	2.562(13)
Pb(2)–O(10)	2.26(2)	Pb(2)–O(11)	2.521(13)
Pb(2)–O(5D)	2.452(15)	Pb(2)–O(15C)	2.511(14)
Pb(3)–O(14)	2.437(13)	Pb(3)–O(13)	2.524(15)
Pb(3)–O(18)	2.469(15)	Pb(3)–O(19)	2.715(15)
Pb(2)–O(12B)	2.553(14)		
O(1)–Pb(1)–O(2)	52.2(4)	O(2)–Pb(1)–O(8)	78.7(5)
O(1)–Pb(1)–O(4A)	75.5(4)	O(4A)–Pb(1)–O(8)	132.0(5)
O(9)–Pb(1)–O(1)	74.7(5)	O(2)–Pb(1)–O(9)	88.3(5)
O(9)–Pb(1)–O(8)	66.6(5)	O(9)–Pb(1)–O(4A)	74.3(5)
O(10)–Pb(2)–O(5D)	73.0(5)	O(10)–Pb(2)–O(15C)	74.7(5)
O(15C)–Pb(2)–O(5D)	147.0(5)	O(3)–Pb(2)–O(11)	154.3(5)
O(3)–Pb(2)–O(10)	78.8(5)	O(3)–Pb(2)–O(5D)	81.0(4)
O(3)–Pb(2)–O(15C)	86.5(5)	O(10)–Pb(2)–O(11)	75.4(6)
O(11)–Pb(2)–O(5D)	90.9(5)	O(11)–Pb(2)–O(15C)	87.2(5)
O(13)–Pb(3)–O(14)	53.0(5)	O(13)–Pb(3)–O(19)	79.8(5)
O(19)–Pb(3)–O(12B)	129.4(5)	O(14)–Pb(3)–O(12B)	77.4(5)
O(18)–Pb(3)–O(14)	74.0(5)	O(13)–Pb(3)–O(18)	86.8(5)
O(18)–Pb(3)–O(19)	66.7(5)	O(18)–Pb(3)–O(12B)	74.8(5)

Symmetry transformation for equivalent atoms: A: $x-1, y, z$; B: $x+1, y, z$; C: $x, y-1, z$; D: $x, y+1, z$

1434 (vs), 1361 (vs), 1219 (s), 1197 (s), 1142 (s), 1107 (s), 1029 (s), 994 (w), 925 (m), 767 (s), 719 (s), 677 (w), 623 (s), 575 (w), 511 (w), 440 (m) cm^{-1}.

X-ray Crystallographic Study: X-ray diffraction data of compound **1** and **2** were collected with a Rigaku Mercury CCD diffractometer equipped with a graphite-monochromated Mo-K_α radiation (λ = 0.71073 Å). The CrystalClear software was used for data reduction and empirical absorption corrections.[48] The structures were solved by direct methods and successive Fourier difference syntheses, and refined by the full-matrix least-squares method on F^2 (SHELXTL Version 5.1[49]). All non-hydrogen atoms except for the carbon atoms of compound **2** were refined with anisotropic thermal parameters. Aromatic hydrogen atoms were assigned to calculated positions with isotropic thermal parameters fixed at 1.2 times that of the attached carbon atom. Hydrogen atoms attached to oxygen atoms for compound **1** were located from difference maps and refined with O–H distances restrained to 0.90 Å, and isotropic thermal parameters fixed at 1.5 times that of the respective oxygen atom. Water hydrogen atoms for compound **2** could not be located in the difference Fourier map. The final Fourier map had a maximum and a minimum electron density of 2.153/–1.675 e·Å^{-3}, 2.438/–3.797 e·Å^{-3} for compound **1** and **2**, respectively, and are within 1.0 Å of the lead atoms. The R_1 values are defined as $R_1 = \Sigma||F_o| - |F_c|| / \Sigma|F_o|$ and $wR_2 = \{\Sigma[w(F_o^2 - F_c^2)^2]/\Sigma[w(F_o^2)^2]\}^{1/2}$. The selected bond lengths and bond angles are listed in Table 2 and details of the crystal parameters, data collection, and refinement are summarized in Table 3.

Table 3. Crystallographic data for compounds **1** and **2**.

	1	**2**
Empirical formula	$C_{16}H_{20}O_{22}S_2Pb_4$	$C_{16}H_{16}O_{19}S_2Pb_3$
Formula mass [g·mol^{-1}]	1457.20	1197.98
Temperature [K]	293(2)	293(2)
Crystal size [mm]	0.12×0.12×0.10	0.24×0.20×0.18
Crystal system	monoclinic	triclinic
Space group	$P2_1/c$	$P\bar{1}$
Z	4	2
a [Å]	13.4123(1)	10.2218(1)
b [Å]	15.2719(1)	10.3214(1)
c [Å]	13.6859(8)	13.315(2)
α [deg]	90	71.866(1)
β [deg]	91.274(3)	71.366(1)
γ [deg]	90	65.06
V [Å^3]	2802.6(3)	1678.07(15)
D_c [g·cm^{-3}]	3.454	3.368
μ [mm^{-1}]	24.203	21.6
Measured reflections	21466	6173
Independent reflections	6398	4144
Observed reflections, [$I > 2\sigma(I)$]	5375	3516
Parameters	436	281
F(000)	2608	1084
Completeness [%]	99.6	98.9
2θ range [°]	3.04 to 27.47	1.65 to 25.04
$h/k/l$ ranges	–16/17	–12/11
	–19/14	–11/12
	–17/17	–15/15
R [int]	0.0524	0.0434
R_1 [obsd. refl.]	0.0495	0.0658
wR_2 [all refl.]	0.0958	0.1523
Largest diff. peak/hole [e·Å^{-3}]	2.153/–1.675	2.438/–3.797

CCDC-285784 (for **1**) and -285785 (for **2**) contain the supplementary crystallographic data for this paper. These data can be obtained free of charge from The Cambridge Crystallographic Data Centre via www.ccdc.cam.ac.uk/data_request/cif.

Supporting Information (for details see the footnote on the first page of this article): This contains the TG curves and X-ray powder diffraction patterns of both compounds.

Acknowledgments

We gratefully acknowledge the financial support of the "One Hundred Talents Program" of the Chinese Academy of Sciences and National Science Foundation of China (Grant No. 20473092).

[1] B. Moulton, M. J. Zaworotko, *Chem. Rev.* **2001**, *101*, 1629–1658.
[2] O. R. Evans, R. Xiong, Z. Wang, G. K. Wong, W. Lin, *Angew. Chem.* **1999**, *111*, 557–559; *Angew. Chem. Int. Ed.* **1999**, *38*, 536–538.
[3] T. Bein, *Supramolecular Architecture*, Am. Chem. Soc. Washington, DC, **1992**.
[4] O. Sato, T. Iyoda, A. Fujishima, K. Hashimoto, *Science* **1996**, *271*, 49–51.
[5] S. K. Ghosh, R. Joan, P. K. Bharadwaj, *Cryst. Growth Des.* **2005**, *5*, 623–629.
[6] D. S. Kim, P. M. Forster, R. L. Toquin, A. K. Cheetham, *Chem. Commun.* **2004**, 2148–2149.
[7] Y. P. Yuan, J. G. Mao, J. L. Song, *J. Solid State Chem.* **2004**, *177*, 922–927.
[8] T. Tsuboi, P. Sifsten, *Phys. Rev. B* **1991**, *43*, 1777–1780.
[9] A. A. Bol, A. Meijerink, *Phys. Chem.* **2001**, *3*, 2105–2112.
[10] P. Singh, M. M. Richter, *Inorg. Chim. Acta* **2004**, *357*, 1589–1592.
[11] S. Miyata, H. S. Nalwa (Eds.), *Organic Electroluminescent Materials and Devices*, Gordon and Breach, New York, **1997**.
[12] C. S. Weinert, I. A. Guzei, A. L. Rheingold, L. R. Sita, *Organometallics* **1998**, *17*, 498–500.
[13] M. H. Jack, M. Saeed, A. S. Ali, *Inorg. Chem.* **2004**, *43*, 1810–1812.
[14] Y. J. Shi, L. H. Li, Y. Z. Li, X. T. Chen, Z. L. Xue, X. Z. You, *Polyhedron* **2003**, *22*, 917–923.
[15] M. R. S. J. Foreman, T. Gelbrich, M. B. Hursthouse, M. J. Plater, *Inorg. Chem. Commun.* **2000**, *3*, 234–238.
[16] R. A. Varga, J. E. Drake, C. Silvestru, *J. Organomet. Chem.* **2003**, *675*, 48–56.
[17] S. M. Ying, J. G. Mao, *Eur. J. Inorg. Chem.* **2004**, 1270–1276.
[18] H. Nikol, A. Vogler, *J. Am. Chem. Soc.* **1991**, *113*, 8988–8990.
[19] R. Ballardini, G. Varani, M. T. Indelli, F. Scandola, *Inorg. Chem.* **1986**, *25*, 3858–3865.
[20] A. Strasser, A. Vogler, *J. Photochem. Photobiol. A* **2004**, *165*, 115–118.
[21] A. Strasser, A. Vogler, *Inorg. Chem. Commun.* **2004**, *7*, 528–530.
[22] D. F. Sun, R. Cao, Y. Q. Sun, X. Li, W. H. Bi, M. C. Hong, Y. J. Zhao, *Eur. J. Inorg. Chem.* **2003**, 94–98.
[23] J. Tao, X. Yin, Z. B. Wei, R. B. Huang, L. S. Zheng, *Eur. J. Inorg. Chem.* **2004**, 125–133.
[24] Z. M. Sun, J. G. Mao, Y. Q. Sun, H. Y. Zeng, A. Clearfield, *Inorg. Chem.* **2004**, *43*, 336–341.
[25] Q. Y. Liu, L. Xu, *Eur. J. Inorg. Chem.* **2005**, 3458–3466.
[26] R. M. Barrer, *Hydrothermal Chemistry of Zeolites*, Academic Press, London, **1982**.
[27] G. Bemazeau, *J. Mater. Chem.* **1999**, *9*, 15–18.
[28] S. H. Feng, R. R. Xu, *Acc. Chem. Res.* **2001**, *34*, 239–247.
[29] F. A. Cotton, G. Wilkinson, *Advanced Inorganic Chemistry*, John Wiley & Sons, New York, **1988**.
[30] T. J. Boyle, T. M. Alam, K. P. Peters, M. A. Rodriguez, *Inorg. Chem.* **2001**, *40*, 6281–6286.
[31] A. Tsohos, S. Dionyssopoulou, C. P. Raptopoulou, A. Terzis, E. G. Bakalbassis, S. P. Perlepes, *Angew. Chem. Int. Ed.* **1999**, *38*, 983–985.
[32] A. V. Sienkiewicz, V. N. Kokozay, *Z. Naturforsch., Teil B* **1994**, *49*, 615–617.

[33] A. V. Sienkiewicz, V. N. Kokozay, *Polyhedron* **1994**, *13*, 1431–1437.
[34] C. D. Brandt, P. G. Pliege, R. J. Kelly, D. J. de Geest, D. K. Kennepohl, S. S. Iremonger, S. Brooker, *Inorg. Chim. Acta* **2004**, *357*, 4265–4272.
[35] Q. Y. Liu, L. Xu, *Inorg. Chem. Commun.* **2005**, *8*, 401–405.
[36] Q. Y. Liu, L. Xu, *Acta Crystallogr., Sect. E* **2005**, *61*, m1972–1974.
[37] G. B. Deacon, R. J. Pihllips, *Coord. Chem. Rev.* **1980**, *33*, 227–250.
[38] S. Deo, H. A. Godwin, *J. Am. Chem. Soc.* **2000**, *122*, 174–175.
[39] P. C. Ford, A. Vogler, *Acc. Chem. Res.*. **1993**, *26*, 220–226.
[40] H. Y. Duan, X. P. Ai, Z. K. He, *Spectrochim. Acta A* **2003**, *60*, 1447–1451.
[41] Y. Q. Xu, D. Q. Yuan, L. Han, E. Ma, M. Y. Wu, Z. Z. Lin, M. C. Hong, *Eur. J. Inorg. Chem.* **2005**, 2054–2059.
[42] Q. Y. Liu, L. Xu, *CrystEngComm* **2005**, *7*, 87–89.
[43] A. Vogler, A. Paukner, H. Kunkely, *Coord. Chem. Rev.* **1980**, *33*, 227–250.
[44] S. K. Dutta, M. W. Perkovic, *Inorg. Chem.* **2002**, *41*, 6938–6940.
[45] H. Kunkely, A. Vogler, *Chem. Phys. Lett.* **1991**, *187*, 609–612.
[46] S. K. Dutta, M. W. Perkovic, *Inorg. Chem.* **2002**, *41*, 6938–6940.
[47] H. Nikol, A. Becht, A. Vogler, *Inorg. Chem.* **1992**, *31*, 3277–3279.
[48] *CrystalClear version 1.3*, Rigaku Corp. **2000**.
[49] G. M. Sheldrick, *SHELXS 97*, *Program for Crystal Structure Solution*, University of Göttingen, **1997**.

Received: October 24, 2005
Published Online: February 24, 2006

